Shock Waves (2017) 27:905–918
DOI 10.1007/s00193-017-0732-x

ORIGINAL ARTICLE

# Efficacy of visor and helmet for blast protection assessed using a computational head model

**D. Singh**[1] · **D. S. Cronin**[1]

Received: 28 October 2016 / Revised: 25 April 2017 / Accepted: 26 May 2017 / Published online: 12 June 2017


**Abstract** Head injury resulting from blast exposure has been identified as a challenge that may be addressed, in part, through improved protective systems. Existing detailed head models validated for blast loading were applied to investigate the influence of helmet visor configuration, liner properties, and shell material stiffness. Response metrics including head acceleration and intracranial pressures (ICPs) generated in brain tissue during primary blast exposure were used to assess and compare helmet configurations. The addition of a visor was found to reduce peak head acceleration and positive ICPs. However, negative ICPs associated with a potential for injury were increased when a visor and a foam liner were present. In general, the foam liner material was found to be more significant in affecting the negative ICP response than positive ICP or acceleration. Shell stiffness was found to have relatively small effects on either metric. A strap suspension system, modeled as an air gap between the head and helmet, was more effective in reducing response metrics compared to a foam liner. In cases with a foam liner, lower-density foam offered a greater reduction of negative ICPs. The models demonstrated the "underwash" effect in cases where no foam liner was present; however, the reflected pressures generated between the helmet and head did not translate to significant ICPs in adjacent tissue, when compared to peak ICPs from initial blast wave interaction. This study demonstrated that the efficacy of head protection can be expressed in terms of load transmission pathways when assessed with a detailed computational model.

Communicated by O. Petel and S. Ouellet.

✉ D. S. Cronin
dscronin@uwaterloo.ca

[1] University of Waterloo, Waterloo, Canada

**Keywords** Blast injury · mTBI · Finite element head model · Helmet protection · Visor

## 1 Introduction and background

The potential for mild traumatic brain injury (mTBI) resulting from blast exposure has received a great deal of attention in recent years, owing to the high rate of incidence observed in recent conflicts. In fact, mTBI was identified as the "signature injury" of military conflicts in Iraq and Afghanistan [1,2], and consequently a large effort was put into understanding and preventing this form of injury.

The potential for brain injury resulting from primary blast exposure, that is the overpressure wave from an explosion, is well established in the literature [3,4]. Although the specific mechanisms of injury are less understood, it has been shown that the isolated pressure wave from a blast event can lead to changes in the cellular function of brain cells, thus indicating the potential for injury [5–8]. A recent study by Sawyer et al. used an advanced blast simulator apparatus to show that primary blast exposure to rats with very small kinematic motion of the head can directly cause changes in brain function [8].

Historically, helmets for military applications have been designed to protect against ballistic impacts from projectiles, and more recently for blunt impact. Modern composite helmets are generally effective against these threats, so the effort has shifted toward increasing protection against blast events. The effect of helmet protection for blast scenarios has been investigated experimentally to some degree in the literature. A physical surrogate head form for experimentally measuring blast response, including head accelerations and intracranial pressures (ICPs), was developed and assessed in free-field blast for the purpose of investigating helmet protection [9–11]. However, it was noted that experimental testing

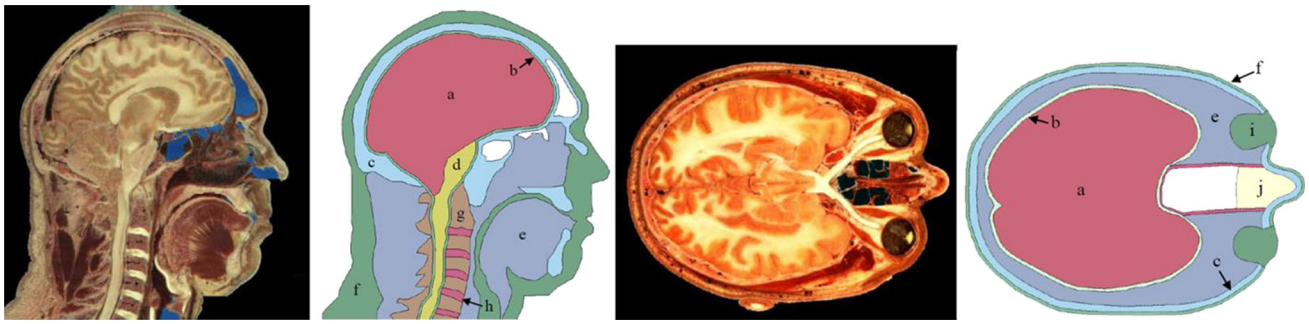


**Fig. 1** Sagittal (*left*) and transverse (*right*) visible human project slices and finite element models showing *a* brain, *b* cerebrospinal fluid, *c* skull, *d* spinal cord, *e* muscle tissue, *f* skin, *g* vertebrae, *h* vertebral disks, *i* eyes, and *j* sinus (soft tissue)

is costly and challenging, such that a computational model could provide significant benefits in identifying promising helmet designs. Dionne et al. reported a reduction in peak head accelerations of 78–84% when comparing helmeted anthropomorphic test devices (ATDs) to unprotected [12].

Finite element methods have been applied to evaluate the effect of helmets on the head and brain response in blast exposures. The addition of a helmet has generally been found to minimally reduce intracranial pressures in the head from frontal blast, although the addition of a visor or face shield provided larger reductions in response metrics [13–16]. Importantly, several studies have reported a phenomenon identified as the "underwash" effect, where an open space between the head and helmet (i.e., no foam liner) allows for pressure wave propagation and reflection between the helmet and head, potentially amplifying the loading to the head [17,18]. The addition of a foam liner reduces this effect, although the liner can also increase the kinematic load on the head due to mechanical coupling between the helmet and the head [17]. For a helmet with a foam liner, the material properties of the foam liner have also been shown to have a significant effect on the intracranial pressures and head accelerations [19,20]. Panzer et al. used a refined planar head model in the transverse plane to look at various helmet liner materials on head kinematics and tissue response and showed that lower-density crushable foams generally improved performance [19]. However, the transverse section in this study included full encirclement of the head, compared to the present study that addressed the facial opening in the helmet. While a number of researchers have contributed importantly to the understanding of the effects of helmets on blast loading, many of these have used finite element models that consist of problematic tetrahedral elements, or elements too coarse to accurately predict brain tissue response in blast.

Mesh convergence studies have identified that an element size of 1 mm is necessary in blast head models to accurately capture the magnitudes of pressure waves [21,22]. Three-dimensional models with this level of mesh refinement, while maintaining continuity between tissue structures, are often computationally prohibitive, particularly for parametric studies, and it has been shown that the planar approximation used in this study provides an accurate prediction of pressures throughout the head, with a possible underprediction of the reflected pressure within the head and opposite to the incident blast wave [22].

One of the most challenging aspects of blast injury research is correlating response with the potential for injury. A number of brain injury metrics have been proposed in the literature as a means of evaluating response, particularly for automotive crash scenarios. In the context of blast related mTBI, the most common metrics are dynamic intracranial pressure, brain tissue shear stress, brain tissue first principal strain, and head acceleration [23,24]. Previous investigations with the head models used in this study have identified dynamic intracranial pressure as providing a measure of tissue-level response [22], while head kinematics [25] are also useful to relate the current results to experimental tests and existing data, where only head kinematics are typically measured.

This study aimed to apply a validated finite element blast head model to assess and explain the efficacy of helmet materials and configurations, gauged through tissue-level response metrics and head kinematics (Fig. 1).

## 2 Methods

The finite element models used in this study are planar models in two perpendicular planes of the head originally developed and validated for head kinematics in free-field blast loading [26], intracranial pressure in shock tube testing of human cadaveric heads [22], and the general effect of helmet liner materials on head response [20]. The current study addresses an important question regarding understanding the importance of coupling the helmet, visor, and liner effects in one model. A commercial explicit finite element code was used in model development (LS-DYNA, R6.1.1, LSTC). The head models are composed of a single layer of 1 mm hexahedral

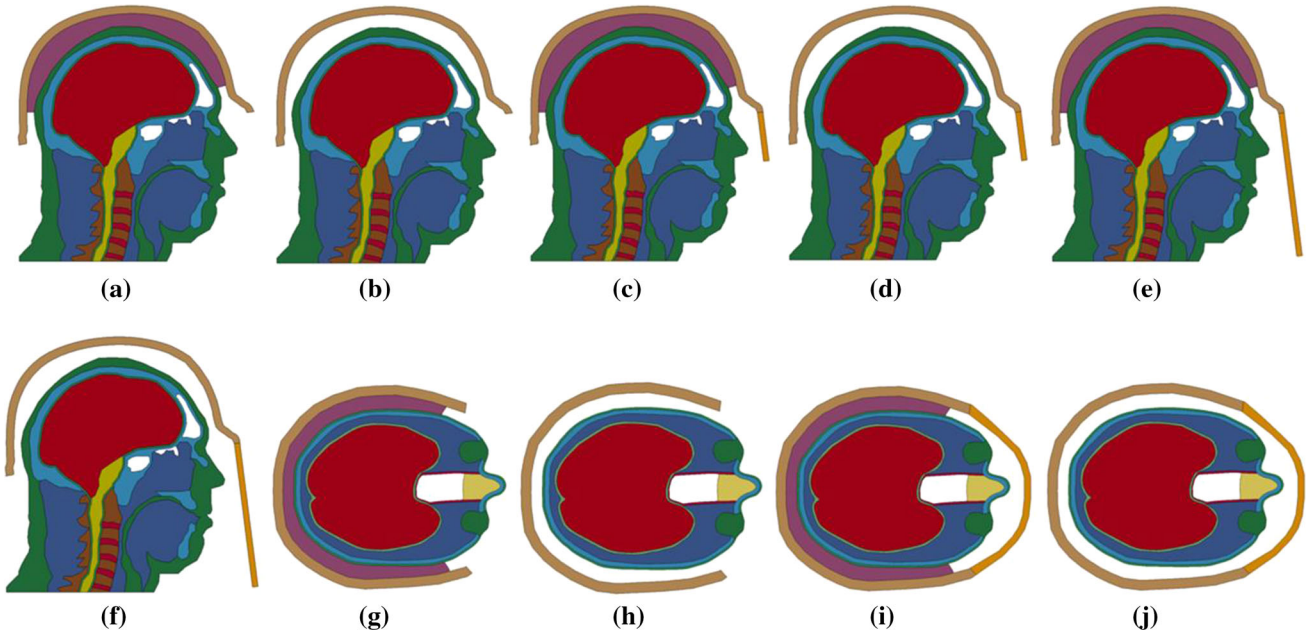


**Fig. 2** Helmet configurations for sagittal **a** no visor with liner, **b** no visor no liner, **c** half visor with liner, **d** half visor no liner, **e** full visor with liner, **f** full visor no liner, and transverse **g** no visor with liner, **h** no visor no liner, **i** with visor with liner, **j** with visor no liner

solid elements in the sagittal and transverse planes of the head (Fig. 2). These models were developed using anatomical slices of a male subject [27], and feature shared nodes between tissues to ensure mesh continuity in order to facilitate stress wave transfer and reflections between tissues in the head.

The sagittal and transverse head models are embedded in an air mesh with an element size of 1 mm in the vicinity of the head models to achieve accurate representation of the coupling and pressure waves, and sized large enough (1.2 m × 2.05 m) to prevent boundary reflections from occurring in the area of interest. Coupling is achieved using a fluid-structure penalty-based algorithm [28]. The air mesh was modeled using Arbitrary Lagrangian Eulerian (ALE) elements, which relocate nodal positions after each time step to prevent element distortion; with material transmitted or advected to adjacent elements using a second-order advection scheme. A boundary is defined around the head model elements where they contact the air, and the code fills the inside of that boundary with a vacuum to prevent the air elements inside the head from contributing to response. This method prevents the need for shared nodes at the air and head interface and is well suited for modeling blast events in air, where element distortions would otherwise become problematic [28,29]. The air mesh requires suitable resolution (∼1 mm in the area of interest) to simulate the peak blast overpressures, and reflected pressures, without excessive "smearing" due to large element sizes. The models and air mesh comprised a total of 206,806 and 183,134 elements for the sagittal and transverse models respectively. The nodes in the models were free to translate and rotate in-plane, and were constrained from out-of-plane translation and rotation.

The head models have been validated using experimental head acceleration for free-field blast exposures (5 kg C-4 at 3, 4, and 5 m standoff) [22,26]. In general, the models were found to predict free-field pressure, reflected pressure and head accelerations in good agreement with the experimental data, assessed using peak values. More recently, the models were assessed using shock tube loading (86–140 kPa overpressure with approximately 6 ms positive phase duration) for experimental tests on human cadaveric heads [30]. The cadaveric experiment produced dynamic intracranial pressure traces for four locations using pressure transducers embedded in the head (frontal, temporal, parietal, and occipital). The head models were exposed to the same loads as the experiment, and the experimental and model response curves were compared using cross-correlation, which is method used to quantify the agreement between curves [22]. The predicted ICPs were in good agreement at the frontal (cross-correlation rating of 0.840), temporal (rating of 0.680), and parietal (rating of 0.610) regions of the brain, and in fair agreement at the occipital regions (rating of 0.400) where three-dimensional superposition effects are exacerbated due to the curvature of the skull [22].

To apply the blast load to the head models, a boundary condition (relative volume and temperature) was prescribed to the leading edge of the air (ALE) mesh, corresponding to the strength and duration of the desired pressure shock wave. The blast load was assumed to be a planar wave with no ground interaction, with the standard Friedlander wave

shape. Two blast load cases, corresponding to a charge size of 5 kg of C4 at 4 and 3 m standoff distance, were used to perform the analysis. These load cases are relevant to mTBI in terms of overpressure magnitude (170 and 326 kPa with positive phase durations of 3.7 and 3.2 ms for the 4 and 3 m standoffs, respectively). For reference, these load cases are equivalent in terms of incident pressure magnitude to a standard US M107 155 mm artillery shell (5.74 kg TNT) blast at standoff distances of between 3.6 and 4.8 m. The resolution of the air mesh was previously verified using experimental data, and in the current study by confirming the magnitude of the applied incident blast waves.

To investigate the effects of helmet protection for blast exposure, the sagittal and transverse models were equipped with various helmet materials (two helmet shell stiffnesses, two liner materials) and configurations (no visor, half visor, full visor) in a parametric study. The helmet geometry was modeled as the PASGT (Personnel Armor System for Ground Troops) helmet design, due to the availability of geometry and material properties, and widespread adoption in military helmet standards. The minor differences in surface geometry between the PASGT helmet and other more recent combat helmets are not expected to have a large effect on head kinematics and outcome. Further, it has been well established that the helmet and visor materials remain elastic during the level of blast exposures considered in this study and in the absence of projectile or fragment impact. The interface between the helmet and the head models did not have shared nodes, but rather a penalty-based contact algorithm (friction coefficient of 0.1) was defined to enable separation of the surfaces for tension loading across the interface. The helmet geometry was modeled using cross-sectional geometries of the PASGT helmet (nominal shell thickness of 9 mm), and was fitted to the head models to represent a snug fit. The element size of the helmet model was also maintained at 1 mm, in agreement with previous convergence studies. In addition to the base helmet geometry, a 6 mm polycarbonate visor was investigated in full-visor and half-visor configurations (Fig. 2). In the transverse model, the full-visor and half-visor configurations are combined into a single visor configuration, due to the nature of the transverse plane.

Two sets of constitutive properties were investigated for the helmet liner, typically polymeric foam, and the helmet shell, typically laminated aramid, to provide a representative range of properties based on previous studies [20,31,32]. The model was also run with no foam liner, to represent a helmet with a strap suspension system. The full parametric study including blast load cases, material property variations, visor configurations, and differentiating between the sagittal and transverse models, resulted in 60 individual cases (case summary found in the Appendix).

The two foam materials assessed for the helmet liner were a high-density and a low-density polyethylene foam, since foam liner density has been reported to be a significant factor influencing helmet effectiveness, in the context of blunt impact. The specific foams were selected to represent a range of density and stiffness that are relevant to combat helmet liners [20]. The foam materials were modeled using a rate-dependent foam constitutive model [20,33].

The baseline helmet shell was modeled as laminated aramid (K29 Kevlar®), a commonly used material in combat helmets with known material properties [32]. To investigate the effects of helmet shell stiffness, a lower stiffness material comparable to the stiffness of ultra-high-molecular-weight polyethylene, was also used, to provide a comparative response to the aramid material. The shell materials were modeled using an orthotropic elastic constitutive model. The polycarbonate visor was modeled using a linear elastic material. A summary of all constitutive properties used in the modeling is shown in Table 1.

The predicted ICP and peak head accelerations for the various load and helmet cases were compared to identify the efficacy of the helmet designs relative to the unprotected case and a standard helmet design. Intracranial pressure, measured as the dynamic ICP from the model, was used as the tissue-level response metric because it has been shown to be a more sensitive metric in blast head injury than brain tissue strain, which is generally low in blast scenarios [22]. Head accelerations were measured using the resultant linear acceleration of the whole skull, due to its relative rigidity compared to the softer tissues of the head.

## 3 Results and discussion

The applied incident blast wave propagated through the ALE air mesh and interacted with the head model for the unprotected case, generating a reflected wave in the surrounding air and a transmitted wave in the affected tissues of the head model. The resulting transmitted pressure waves in the head propagate and reflect between the various tissue layers in the head model, producing transient dynamic pressure and therefore stresses and strains in the brain tissue (Fig. 3). For the unprotected case, in the sagittal model, the frontal region of the brain is initially insulated from the blast wave by the air-filled sinus cavity, so the wave travels through the facial tissues and the skull and transmits into the brain both above and below the sinus cavity. Similarly in the unprotected transverse model, the anterior portion of the brain is protected by the sinus cavity, although some of the energy of the wave is transferred through the bone surrounding the sinus to load the brain tissue directly. The soft tissue pathway through the eyes serves as a secondary load transmission pathway to the brain. Some wrapping of the blast wave under the neck is observed in the sagittal model where the false boundary condition at the inferior terminus of the cervical spine causes

**Table 1** Constitutive properties for all materials used in the modeling [22,32–34]

| Tissue | Material model | Density ($kg/m^3$) | Poisson's ratio | Modulus (GPa) | Viscoelastic properties | Viscosity ($\mu Pa \cdot s$) | Ideal gas properties |
|---|---|---|---|---|---|---|---|
| Air | Ideal gas | 1.205 | | | | 18.21 | $C_{V0} = 717.86$ |
| | | | | | | | $C_{P0} = 1005$ |
| | | | | | | | $C_L = 0$ |
| | | | | | | | $C_O = 0$ |
| | | | | | | | $T_0 = 295.15$ |
| | | | | | | | $V_0 = 1.0$ |
| Skull/vertebrae | Elastic | 1561 | 0.379 | $E = 7.92$ | | | |
| Vertebral disks | Elastic | 1040 | 0.40 | $E = 0.0034$ | | | |
| Skin | Elastic | 1040 | 0.42 | $E = 1.7$ | | | |
| Muscle/skin | Hyperelastic | 1050 | | $K = 2.2$ | | | |
| CSF | Fluid | 1040 | | $K = 2.2$ | | | |
| Brain | Hyper-viscoelastic | 1040 | | $K = 2.2$ | $G_\infty = 15.9$ kPa | | |
| | | | | | $G_0 = 0.36$ kPa | | |
| | | | | | $\beta = 504.5\ s^{-1}$ | | |
| Foam (low density) | Rate-dependent foam | 45 | | $E = 0.00032$ | | | |
| Foam (high density) | Rate-dependent foam | 80 | | $E = 0.00272$ | | | |
| Shell material (low stiffness) | Orthotropic | 1230 | | $E_1 = 1.85$ | | | |
| | | | $\nu_{21} = 0.25$ | $E_2 = 1.85$ | | | |
| | | | $\nu_{31} = 0.33$ | $E_3 = 0.6$ | | | |
| | | | $\nu_{32} = 0.33$ | $G_{12} = 0.077$ | | | |
| | | | | $G_{23} = 0.543$ | | | |
| | | | | $G_{31} = 0.543$ | | | |
| Shell material (high stiffness) | Orthotropic | 1230 | | $E_1 = 18.5$ | | | |
| | | | $\nu_{21} = 0.25$ | $E_2 = 18.5$ | | | |
| | | | $\nu_{31} = 0.33$ | $E_3 = 6$ | | | |
| | | | $\nu_{32} = 0.33$ | $G_{12} = 0.77$ | | | |
| | | | | $G_{23} = 5.43$ | | | |
| | | | | $G_{31} = 5.43$ | | | |
| Polycarbonate | Elastic | 1200 | 0.37 | $E = 2.3$ | | | |

some unphysical loading of the lower part of the neck tissues. However, this effect is remote to the brain and does not extend to the brain tissue regions in the model during the timeframe of the simulation.

The resulting maximum intracranial pressures and head accelerations were extracted from the model results for each case and compared to the unprotected case. To prevent single elements from dominating the intracranial pressure response, the 5% maximum volume fraction values of intracranial pressure were used in this averaging as per Singh et al. [22]. This is defined as the greatest magnitude of intracranial pressure that at least 5% of the brain tissue volume was exposed to. The threshold of 5% was deemed adequate to provide a good representative value and did not affect any of the observed trends.

The results of the parametric study for the sagittal (Table 2) and transverse (Table 3) models for the 4 m standoff case were compared to identify the efficacy of the various configurations. In these tables, the percent reduction is reported as positive where the protected configuration resulted in a decrease in response magnitude, and vice-versa. In terms of peak head acceleration, there was a clear reduction in the sagittal model response for the helmet-protected cases compared to the unprotected case. The peak head accelerations were reduced by an average of 30, 53, and 82% in the cases with no visor, half visor, and full visor, respectively (Table 2). In the transverse model, no reduction in acceleration was observed for the helmet-protected case with no visor, while reductions of 27–58% were seen in the case with the visor. Furthermore, the transverse model reported mod-

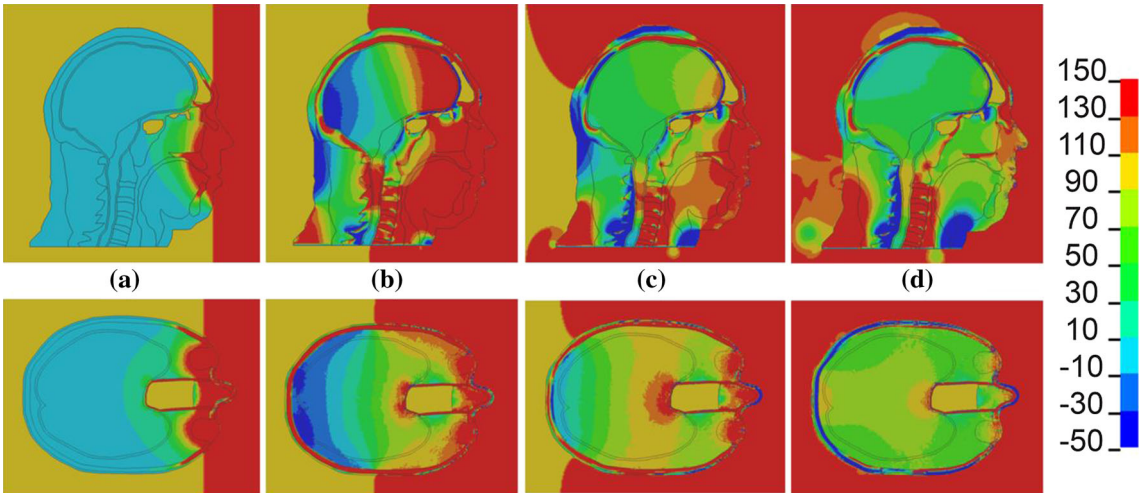


**Fig. 3** Contours of pressure (kPa) for the unprotected sagittal (*top*) and transverse (*bottom*) models at **a** 0.60 ms, **b** 0.86 ms, **c** 1.12 ms, and **d** 1.35 ms

**Table 2** Parametric study results for sagittal model at 4 m standoff (% reduction = [(unprotected − current)/unprotected] * 100%)

| Configuration | | | ICP (Pa) | | Negative ICP (Pa) | | Head acceleration (1000 m/s$^2$) | |
|---|---|---|---|---|---|---|---|---|
| Visor | Foam | Kevlar | 5% Max | % Reduction | 5% Max | % Reduction | Peak | % Reduction |
| Unprotected | | | 174,500 | | 34,700 | | 1.44 | |
| None | High $\rho$ | Low $E$ | 134,300 | 23.0 | 19,500 | 43.8 | 1.006 | 30.1 |
| None | High $\rho$ | High $E$ | 135,500 | 22.3 | 25,000 | 28.0 | 1.006 | 30.1 |
| None | Low $\rho$ | Low $E$ | 133,000 | 23.8 | 19,800 | 42.9 | 0.996 | 30.8 |
| None | Low $\rho$ | High $E$ | 137,000 | 21.5 | 25,800 | 25.6 | 1.026 | 28.8 |
| None | None | Low $E$ | 128,800 | 26.2 | 100 | 99.7 | 0.969 | 32.7 |
| None | None | High $E$ | 131,000 | 24.9 | 5400 | 84.4 | 1.009 | 29.9 |
| Half | High $\rho$ | Low $E$ | 108,300 | 37.9 | 25,000 | 28.0 | 0.652 | 54.7 |
| Half | High $\rho$ | High $E$ | 110,800 | 36.5 | 26,500 | 23.6 | 0.647 | 55.1 |
| Half | Low $\rho$ | Low $E$ | 109,000 | 37.5 | 25,000 | 28.0 | 0.641 | 55.5 |
| Half | Low $\rho$ | High $E$ | 127,500 | 26.9 | 12,800 | 63.1 | 0.704 | 51.1 |
| Half | None | Low $E$ | 122,300 | 29.9 | 100 | 99.7 | 0.681 | 52.7 |
| Half | None | High $E$ | 131,000 | 24.9 | 3300 | 90.5 | 0.742 | 48.5 |
| Full | High $\rho$ | Low $E$ | 85,500 | 51.0 | 58,000 | −67.1 | 0.318 | 77.9 |
| Full | High $\rho$ | High $E$ | 86,800 | 50.3 | 55,300 | −59.4 | 0.311 | 78.4 |
| Full | Low $\rho$ | Low $E$ | 80,500 | 53.9 | 40,200 | −15.9 | 0.279 | 80.6 |
| Full | Low $\rho$ | High $E$ | 83,500 | 52.1 | 32,800 | 5.5 | 0.276 | 80.8 |
| Full | None | Low $E$ | 62,500 | 64.2 | 100 | 99.7 | 0.193 | 86.6 |
| Full | None | High $E$ | 69,800 | 60.0 | 2100 | 93.9 | 0.204 | 85.8 |

erate differences in the visor-protected cases depending on the foam material (Table 3). The no foam case reported the greatest reduction (average of 57%), followed by the low-density foam (average of 45%) and the high-density foam (average of 28%).

In terms of intracranial pressure, the sagittal model identified a reduction in the positive ICPs for all helmet-protected cases, with the greatest reduction in the full visor case (Table 2). In the transverse model, a slight increase (average of 18%) in the positive ICPs was observed in the helmet-protected case with no visor, while a large reduction (average of 93%) is seen in the visor-protected case (Table 3). In both the sagittal and transverse models, the full visor with no foam resulted in the greatest reduction of positive ICPs.

Many previous studies have reported the occurrence of negative ICP within the CSF and brain tissue, attributed to the reflection of the incident compression wave opposite the exposed side of the head. Considering negative ICP, the sagittal model reported reductions in magnitude for the no visor and half visor cases, with the greatest reduction for the no

**Table 3** Parametric study results for transverse model at 4 m standoff (% reduction = [(unprotected − current)/unprotected] * 100%)

| Configuration | | | ICP (Pa) | | Negative ICP (Pa) | | Head acceleration (1000 m/s$^2$) | |
|---|---|---|---|---|---|---|---|---|
| Visor | Foam | Kevlar | 5% Max | % Reduction | 5% Max | % Reduction | Peak | % Reduction |
| Unprotected | | | 148,500 | | 28,200 | | 1.82 | |
| None | High $\rho$ | Low $E$ | 178,000 | −19.9 | 24,900 | 11.7 | 1.825 | −0.3 |
| None | High $\rho$ | High $E$ | 171,000 | −15.2 | 33,500 | −18.8 | 1.918 | −5.4 |
| None | Low $\rho$ | Low $E$ | 176,000 | −18.5 | 24,000 | 14.9 | 1.831 | −0.6 |
| None | Low $\rho$ | High $E$ | 155,000 | −4.4 | 55,500 | −96.8 | 2.089 | −14.8 |
| None | None | Low $E$ | 183,500 | −23.6 | 10,500 | 62.8 | 1.674 | 8.0 |
| None | None | High $E$ | 184,500 | −24.2 | 21,800 | 22.7 | 1.82 | 0.0 |
| Full | High $\rho$ | Low $E$ | 8,200 | 94.5 | 136,000 | −382.3 | 1.28 | 29.7 |
| Full | High $\rho$ | High $E$ | 10,200 | 93.1 | 151,800 | −438.3 | 1.335 | 26.6 |
| Full | Low $\rho$ | Low $E$ | 22,000 | 85.2 | 90,500 | −220.9 | 1.038 | 43.0 |
| Full | Low $\rho$ | High $E$ | 14,600 | 90.2 | 99,000 | −251.1 | 0.967 | 46.9 |
| Full | None | Low $E$ | 3120 | 97.9 | 4050 | 85.6 | 0.763 | 58.1 |
| Full | None | High $E$ | 2510 | 98.3 | 4250 | 84.9 | 0.811 | 55.4 |

foam configurations (Table 2). For the sagittal full visor case, the no foam configuration resulted in a large reduction (average of 97%) in negative ICPs, however the configurations with a foam liner identified increased negative ICPs (average of 5 and 63% increase for the low-density and high-density foam liner respectively, Table 3). This increase was attributed to the full visor preventing a large part of the compressive incident wave from transmitting directly into the facial tissues, where it would otherwise superimpose and mitigate some of the tensile reflection at the back of the head. In the transverse model, the helmet-protected case with no visor protection reported large variations in negative ICP response for each configuration. The high-density helmet shell material resulted in greater reductions for the configurations with a foam liner, although the no foam configuration resulted in the greatest reductions. In the visor-protected configuration, the foam liner resulted in large increases in the negative ICP response, in agreement with the sagittal model. The visored case with no foam liner resulted in the greatest negative ICP reductions (average of 85%) in the transverse model (Table 3). The greatest negative ICPs are generated opposite the initial wave impact, at the occipital regions of the brain, where the helmet shell and liner materials have a stronger influence on response. Consequently, the foam lining and helmet shell material play a more significant role in the negative ICP response, as opposed to positive ICP or head acceleration.

### 3.1 Pathways of loading for helmet protection

The model results demonstrate differences in load transmission pathways to the brain tissue for the various configurations considered (Fig. 4). In the helmet-protected sagittal model with a foam liner and no visor, there are two main pathways of loading of the incident pressure wave to the brain, through the facial tissues and through the helmet foam (Fig. 4a). In this particular case, the pathways combine quickly due to the close proximity and lack of obstacles to the wave with no visor present. The greatest positive ICPs are generated near the sinuses at the frontal lobe, and the greatest negative ICPs are generated at the occipital lobe as the compressive wave is reflected in tension at the back of the head.

Without the foam liner, the transmission path from the foam is eliminated, so the primary pathway is through the facial tissues (Fig. 4b). However, the pressure wave is able to propagate and reflect in the space between the helmet and the head (described as underwash), which results in a moderate increase in ICP along the parietal and occipital regions of the brain.

In the sagittal model with a half visor, the load transmission pathways are similar to the no visor case. The half visor deflects some of the incident wave near the eyes and nose, but a large area of the facial tissues are exposed, so the wave transmission through these tissues is not significantly obstructed (Fig. 4c, d).

In the sagittal model with a foam liner and a full visor, the brain tissue is first loaded at the forehead region from the compression of the helmet foam material near the forehead. At the same time, the wave propagates around the bottom aspect of the visor and enters the facial tissues (Fig. 4e). The result is a reduction in the positive ICPs at the frontal regions of the brain, and an increase in the negative ICPs at the occipital regions, due to the time delay and the dispersal of the large proportion of the incident wave that was blocked by the visor. The sagittal model with no foam liner and a full visor,

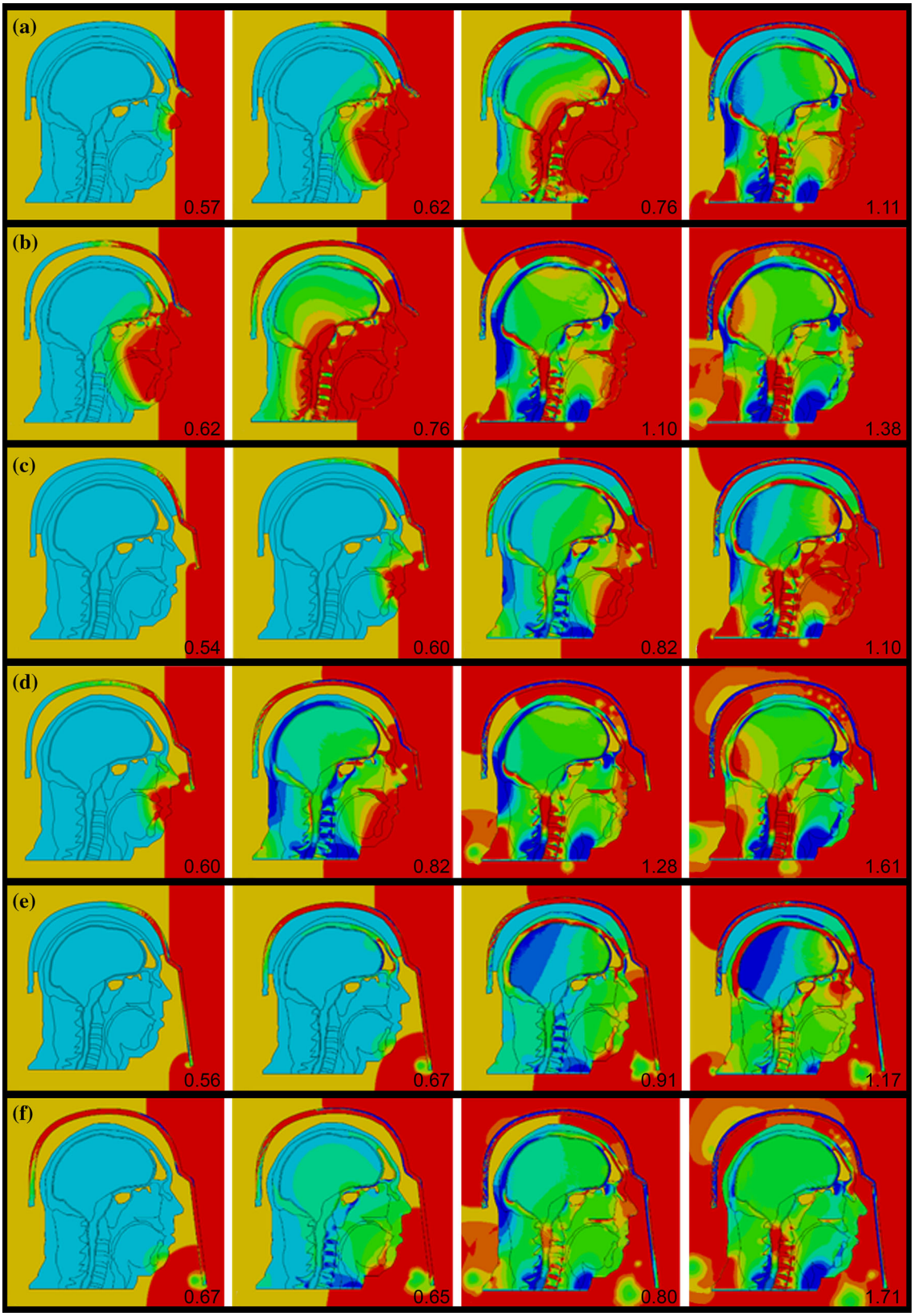


**Fig. 4** Contours of pressure (refer to Fig. 3 for contour scale) of sagittal model with **a** no visor and foam lining, **b** no visor and no foam lining, **c** half visor and foam lining, **d** half visor and no foam lining, **e** full-visor and foam lining, **f** full-visor and no foam lining. The simulation time (ms) is shown at the *bottom right* of each image

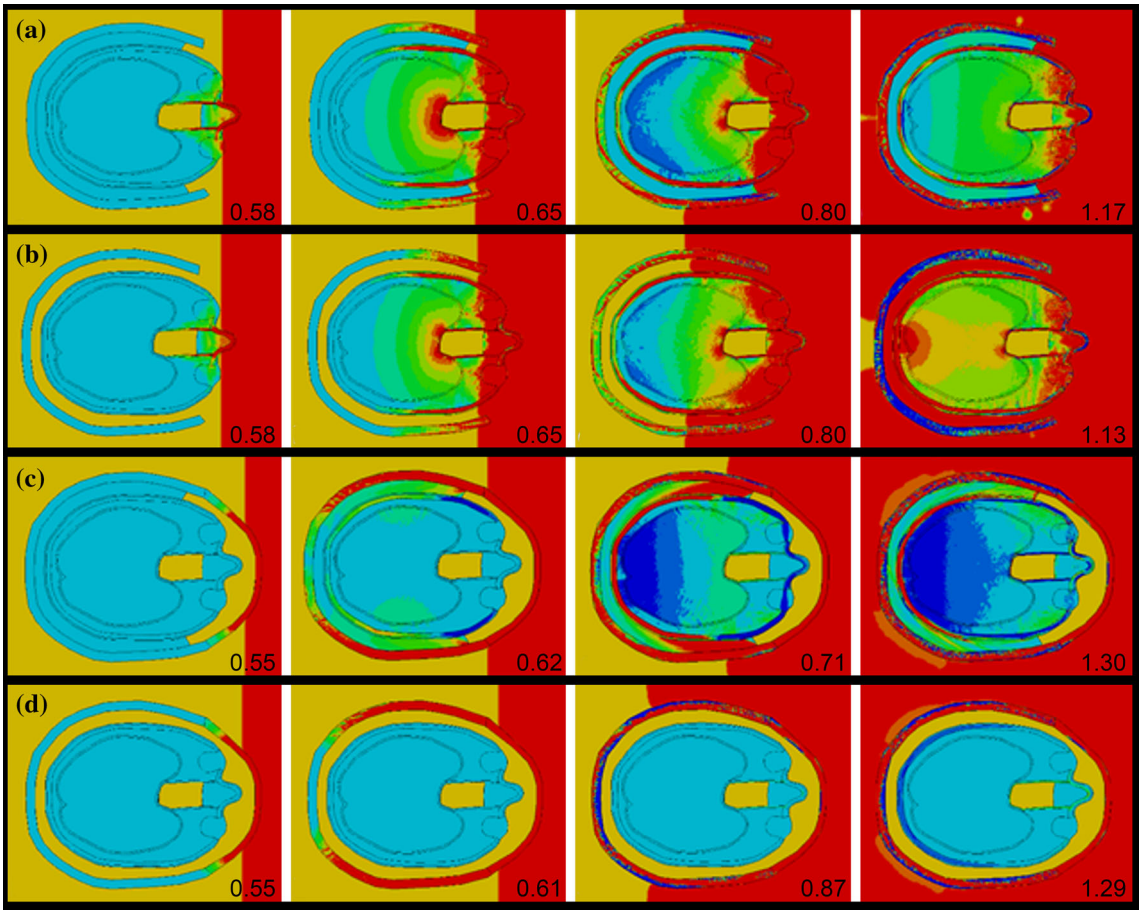


**Fig. 5** Contours of pressure (refer to Fig. 3 for contour scale) of transverse model with **a** no visor and foam lining, **b** no visor and no foam lining, **c** full-visor and foam lining, **d** full-visor and no foam lining. The simulation time (ms) is shown at the *bottom right* of each image

the pathway of loading is solely from the portion of the wave that wraps around the bottom aspect of the visor and loads the facial tissues (Fig. 4f). Wave reflections between the helmet and the head were observed, although in this case did not produce corresponding regions of greater ICP in the adjacent brain tissue, as was observed in the no foam configuration with no visor. Based on this observation, the additional wave travel distance required by the presence of a full visor, as compared to no visor or a half visor, mitigates the increase in ICPs due to the underwash phenomenon.

In the transverse model with a foam liner and no visor, the pathway of loading to the brain tissue was directly through the facial tissues (Fig. 5a). The brain tissue is initially exposed to compressive loading at the frontal regions, and then a negative pressure loading at the occipital regions as the compressive wave reflects in tension. With no foam liner, the load pathway is the same, although there is a distinct high ICP region produced in the occipital region later in time as the pressure wave propagates between the helmet and the head (Fig. 5b), similar to the effect observed in the helmeted sagittal model with no foam.

In the transverse model with a foam liner and a visor, the incident wave is reflected by the visor and has to transmit through the helmet and liner, thereby creating modest ICP at the temporal regions, followed by negative pressures at the occipital regions (Fig. 5c). When the foam liner is removed, the head is essentially decoupled from the helmet in the transverse model, which greatly reduces the loading on the brain tissue and ICP (Fig. 5d).

### 3.2 Parameter effects

The average values of peak intracranial pressure, peak negative intracranial pressure, and peak head acceleration for all the helmet-protected cases were compared for each variable in the parametric study.

The presence of a visor had a significant effect on both ICP predictions and head acceleration (Fig. 6). Both the sagittal and transverse models demonstrate a clear reduction in peak head acceleration and positive intracranial pressure as the visor size increases. The sagittal model reported an average reduction in peak head acceleration of 33 and 78% for the

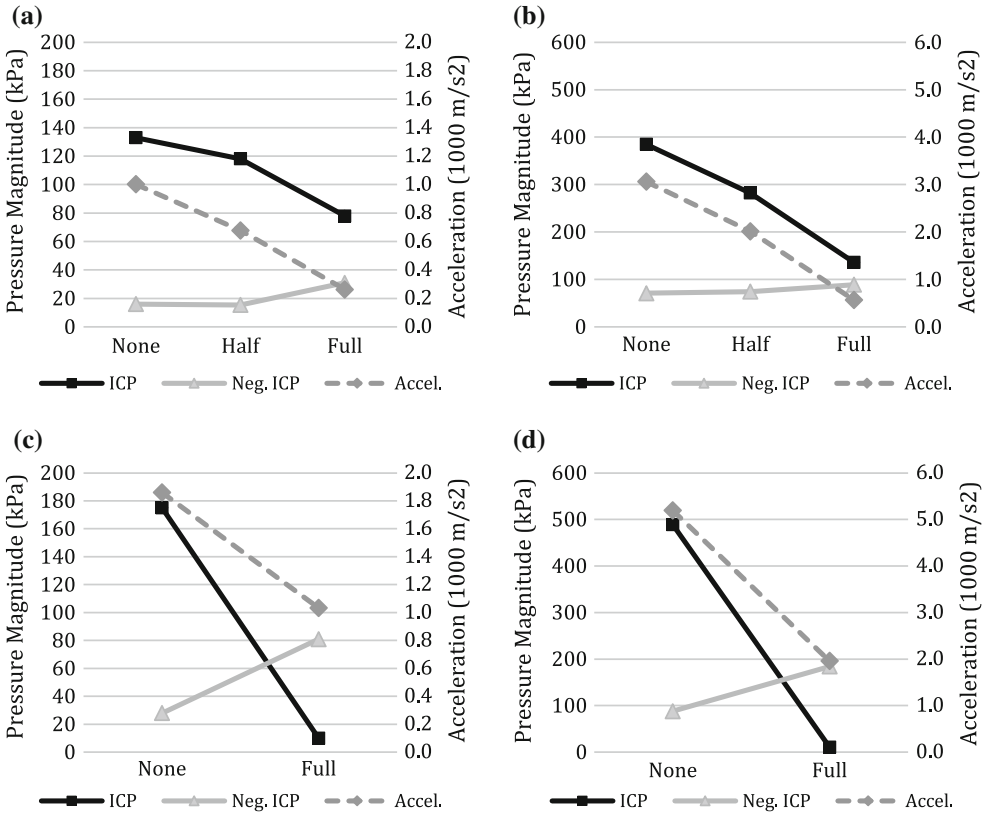


**Fig. 6** Visor configuration averages for **a** sagittal model at 4 m, **b** sagittal model at 3 m, **c** transverse model at 4 m, and **d** transverse model at 3 m

half visor and full visor respectively. In the transverse model, the accelerations were reduced by 53% with a visor. For positive ICP, the sagittal model reported reductions of 19 and 53% for the half visor and full visor respectively, while the transverse model reported a reduction of 96% with a visor. In contrast, the negative intracranial pressure increased with a visor, by 34 and 59% for the sagittal and transverse models respectively.

The results from comparing the foam materials also demonstrate some important trends (Fig. 7). Overall, the differences in positive intracranial pressure were small for the different foam materials compared to the effect of the visor. In their study, Panzer et al. found more significant differences in response comparing different foam materials; however, their model of the transverse plane of the head was fully enclosed by a helmet and padding [19], whereas the model in this study includes padding approximately 2/3 up the sides of the head. In a fully enclosed configuration, it would be expected that the foam liner material could play a more significant role in head response. The sagittal model demonstrated an important difference in the trend with regard to the blast load case. In the 4 m standoff load case, the positive ICP was slightly lower (by 4%) in the case with no foam liner, whereas the 3 m standoff load case showed a slight increase (by 4%) in positive ICP with no foam liner (Fig. 7). This is due to the increased effect of reflected pressures, which is known to be non-linear, between the helmet and the head as the blast load intensity increases. The negative ICPs in both models were lowest in the case with no foam liner, and greatest in the case with the high-density foam. In terms of peak head acceleration, the sagittal model demonstrated a similar trend to the positive ICP in that the no foam case resulted in a slight reduction in head acceleration for the 4 m load case, and a slight increase for the 3 m load case. In the transverse model, the high-density foam resulted in the greatest head accelerations, followed by the low-density foam, and then the no foam case.

Relatively small differences in the average values of intracranial pressure and head acceleration were observed when comparing the helmet shell material stiffness (Fig. 8), compared to the effects of the visor and foam material. The sagittal model reported marginally smaller ICP for the high stiffness shell, with no effect on negative ICP or acceleration. The largest observed trend for helmet shell stiffness was the negative ICP in the transverse model, where the high stiffness shell reported 20% lower negative ICPs.

## 4 Conclusions

Two finite element blast head models, with geometries in the sagittal and transverse planes, were applied to investi-

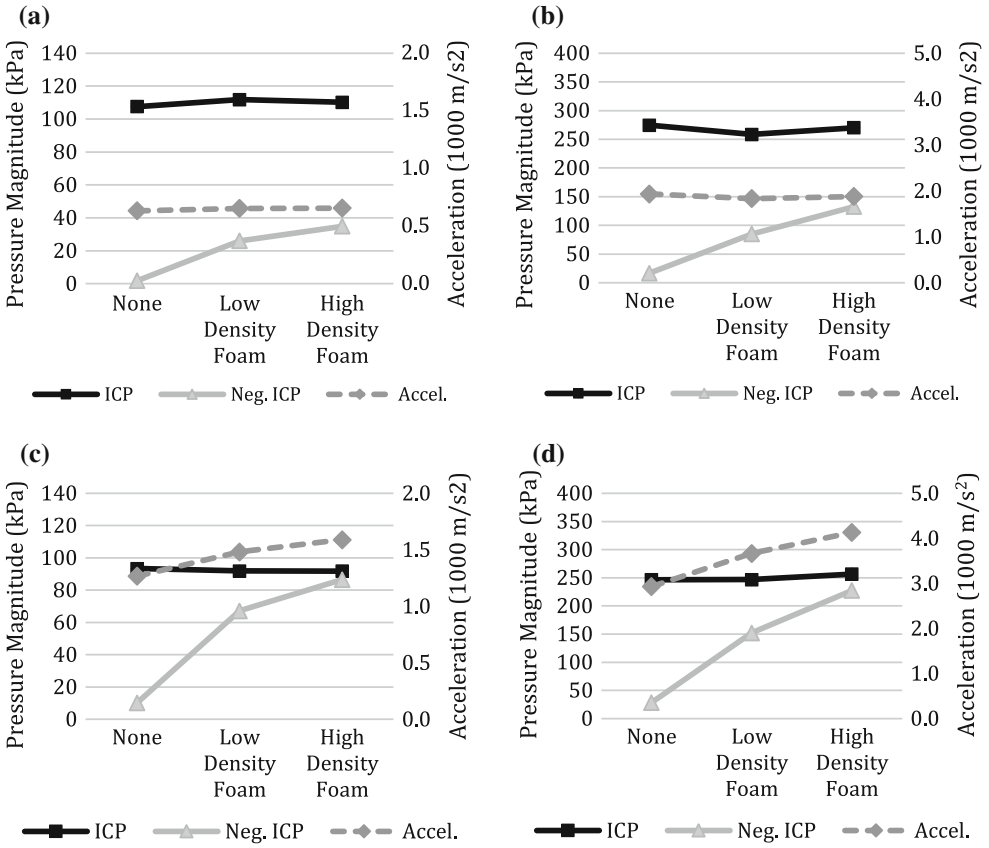


**Fig. 7** Foam material averages for **a** sagittal model at 4 m, **b** sagittal model at 3 m, **c** transverse model at 4 m, and **d** transverse model at 3 m

gate the influence of helmet visors, foam liner presence and density, and helmet material stiffness, on the head acceleration and intracranial pressures generated in brain tissue during primary blast exposure. The major limitation of this work is the lack of three-dimensional effects captured by the models, which has been shown to affect intracranial pressures at the occipital regions of the brain [22]. Only the head was modeled, so an artificial boundary was introduced at the neck. Furthermore, the scope of the current study was limited to primary blast exposure, so secondary or tertiary blast effects later in time were not considered. These limitations underscore the computational challenges inherent to modeling complex blast interactions, where appropriate mesh size and tissue continuity are critical. Nevertheless, the models provide a reasonable means of comparing responses between different helmet configurations, and observing trends.

The peak head accelerations were predicted to decrease with the presence of a visor in both the sagittal and transverse models. The additional mass and the deflection of the incident wave provided by the visor contributed to this reduction. Decreased head acceleration with the presence of the helmet is in agreement with previous studies that have investigated this issue [13,19,20]. The positive intracranial pressures were significantly reduced with the addition of a half-visor, and more so with a full-visor, as expected and in agreement with previous studies [14–16]. Interestingly however, the negative ICPs were increased in the full visor cases. This was attributed to, firstly, the visor concentrating more of the incident wave to the forehead region of the head, where it was able to propagate through the brain tissue and reflect in tension, generating negative pressures. And secondly, in contrast to the half-visor and no visor cases, the full visor obstructs the remainder of the incident wave from transmitting into the head through the face, which mitigates some of the tensile reflection through superposition. This effect was not observed in the cases with no foam liner, since the air gap between the head and the helmet prevented any substantial wave transmission from the helmet to the head. In general, a half-visor was about half as effective in mitigating peak head accelerations and peak positive ICPs in the brain as a full-visor, and had no significant effect on negative ICPs as compared to a helmet with no visor.

The foam liner was found to have the most significant effect on the negative ICP, where the no foam configuration reported the lowest magnitude negative ICPs, followed by the low-density foam and then the high-density foam. In contrast to positive pressures which are generally occurring at the exposed surface of the head (anterior in this study),

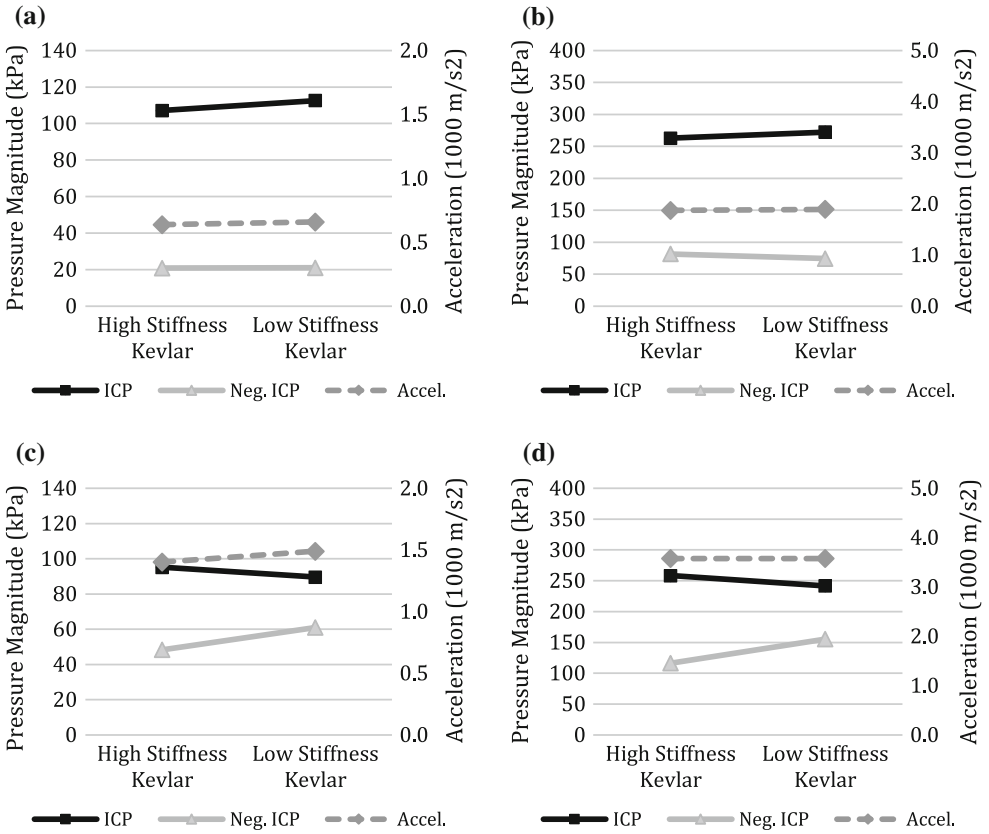


**Fig. 8** Kevlar material averages for **a** sagittal model at 4 m, **b** sagittal model at 3 m, **c** transverse model at 4 m, and **d** transverse model at 3 m

the greatest negative pressures affect the occipital regions of the brain, where the foam material has a stronger influence on wave behavior. In the no foam case, the portion of the wave that is transmitted into the helmet shell is decoupled from the head, so its contribution to the loading on brain tissue is eliminated, thereby reducing the pressures. Moreover, the lower-density foam reduced the negative pressures more so than the high-density foam due to the greater impedance mismatch between the low-density foam and helmet shell material, which reduced the amount of wave transmission that could occur. The helmet shell stiffness was not found to have a significant effect. It should be noted that the foam pad system may be of benefit for head protection in blunt impact, so future studies should also consider this mode of loading when optimizing a helmet design; however, this was beyond the scope of the current study.

Both the sagittal and transverse models demonstrated the "underwash" effect in the cases where no foam liner was present, where the blast wave was able to propagate and reflect in the air gap between the head and the helmet. These reflections did generate moderate ICPs in the adjacent brain tissue in the no visor and half visor cases; however, the magnitude of these generated ICPs were generally lower than the peak ICPs at the frontal regions of the brain during initial impact of the blast pressure wave.

This study presented a parametric study on some aspects of helmet design and how they affect relevant measures of head response in primary blast. Ultimately, head protection must meet a number of criteria including blunt impact, ballistic impact and blast exposure. In the case of blast exposure, the most effective means of reducing the head response metrics considered was the addition of a full visor, followed by the utilization of a strap suspension system rather than a foam liner. In cases with a foam liner, a low-density foam was found to be more effective in mitigating response. This study demonstrated that the efficacy of head protection can be expressed in terms of load transmission pathways when assessed with a detailed computational model, and that quantification of response in terms of kinematics and tissue-level response can inform helmet design for blast exposures. Future work can focus on the effects of head orientation, complex blast waves and ground interaction, and optimization of helmet configuration and properties.

**Acknowledgements** The authors would like to acknowledge the support of the Natural Sciences and Engineering Research Council and Compute Canada.

## Appendix: Parametric study case summary

| | Model | | Standoff | | Visor | | | Foam | | | Kevlar | |
|---|---|---|---|---|---|---|---|---|---|---|---|---|
| | Sag. | Trans. | 4 m | 3 m | None | Half | Full | None | Low $\rho$ | High $\rho$ | Low $E$ | High $E$ |
| 1 | X | | X | | X | | | X | | | X | |
| 2 | X | | X | | X | | | X | | | | X |
| 3 | X | | X | | X | | | | X | | X | |
| 4 | X | | X | | X | | | | X | | | X |
| 5 | X | | X | | X | | | | | X | X | |
| 6 | X | | X | | X | | | | | X | | X |
| 7 | X | | X | | | X | | X | | | X | |
| 8 | X | | X | | | X | | X | | | | X |
| 9 | X | | X | | | X | | | X | | X | |
| 10 | X | | X | | | X | | | X | | | X |
| 11 | X | | X | | | X | | | | X | X | |
| 12 | X | | X | | | X | | | | X | | X |
| 13 | X | | X | | | | X | X | | | X | |
| 14 | X | | X | | | | X | X | | | | X |
| 15 | X | | X | | | | X | | X | | X | |
| 16 | X | | X | | | | X | | X | | | X |
| 17 | X | | X | | | | X | | | X | X | |
| 18 | X | | X | | | | X | | | X | | X |
| 19 | X | | | X | X | | | X | | | X | |
| 20 | X | | | X | X | | | X | | | | X |
| 21 | X | | | X | X | | | | X | | X | |
| 22 | X | | | X | X | | | | X | | | X |
| 23 | X | | | X | X | | | | | X | X | |
| 24 | X | | | X | X | | | | | X | | X |
| 25 | X | | | X | | X | | X | | | X | |
| 26 | X | | | X | | X | | X | | | | X |
| 27 | X | | | X | | X | | | X | | X | |
| 28 | X | | | X | | X | | | X | | | X |
| 29 | X | | | X | | X | | | | X | X | |
| 30 | X | | | X | | X | | | | X | | X |
| 31 | X | | | X | | | X | X | | | X | |
| 32 | X | | | X | | | X | X | | | | X |
| 33 | X | | | X | | | X | | X | | X | |
| 34 | X | | | X | | | X | | X | | | X |
| 35 | X | | | X | | | X | | | X | X | |
| 36 | X | | | X | | | X | | | X | | X |
| 37 | | X | X | | X | | | X | | | X | |
| 38 | | X | X | | X | | | X | | | | X |
| 39 | | X | X | | X | | | | X | | X | |
| 40 | | X | X | | X | | | | X | | | X |
| 41 | | X | X | | X | | | | | X | X | |
| 42 | | X | X | | X | | | | | X | | X |
| 43 | | X | X | | | | X | X | | | X | |
| 44 | | X | X | | | | X | X | | | | X |
| 45 | | X | X | | | | X | | X | | X | |
| 46 | | X | X | | | | X | | X | | | X |
| 47 | | X | X | | | | X | | | X | X | |
| 48 | | X | X | | | | X | | | X | | X |
| 49 | | X | | X | X | | | X | | | X | |
| 50 | | X | | X | X | | | X | | | | X |
| 51 | | X | | X | X | | | | X | | X | |
| 52 | | X | | X | X | | | | X | | | X |
| 53 | | X | | X | X | | | | | X | X | |
| 54 | | X | | X | X | | | | | X | | X |
| 55 | | X | | X | | | X | X | | | X | |
| 56 | | X | | X | | | X | X | | | | X |
| 57 | | X | | X | | | X | | X | | X | |
| 58 | | X | | X | | | X | | X | | | X |
| 59 | | X | | X | | | X | | | X | X | |
| 60 | | X | | X | | | X | | | X | | X |

## References


1. Wojcik, B.E., Stein, C.R., Bagg, K., Humphrey, R.J., Orosco, J.: Traumatic brain injury hospitalizations of US army soldiers deployed to Afghanistan and Iraq. Am. J. Prev. Med. **38**(1), S108–S116 (2010). doi:10.1016/j.amepre.2009.10.006
2. Connolly, T.J.M., Clutter, J.K.: Criteria to determine likelihood of brain injury during explosive events. Saf. Sci. **48**(10), 1387–1392 (2010). doi:10.1016/j.ssci.2010.05.013
3. Taber, K.H., Warden, D.L., Hurley, R.A.: Blast-related traumatic brain injury: what is known? J. Neuropsychiatry Clin. Neurosci. **18**(2), 141–145 (2006). doi:10.1176/jnp.2006.18.2.141
4. Gupta, R.K., Przekwas, A.: Mathematical models of blast-induced TBI: current status, challenges, and prospects. Front. Neurol. **4**, 1–21 (2013). doi:10.3389/fneur.2013.00059
5. Effgen, G.B., Ong, T., Nammalwar, S., Ortuño, A.I., Meaney, D.F., Bass, C.R., Barclay III, M.: Primary blast exposure increases hippocampal vulnerability to subsequent exposure: reducing long-term potentiation. J. Neurotrauma **33**, 1901–1912 (2016). doi:10.1089/neu.2015.4327
6. Vogel, E., Villacorta, J., Bass, C.R., Meaney, D.F., Morrison III, B.: Primary blast injury erases long term potentiation in rat brain organotypic hippocampal slices. In: IRCOBI Conference 2014, IRC-14-89. Berlin, Germany (2014)
7. Pham, N., Sawyer, T.W., Wang, Y., Rastgar Jazii, F., Vair, C., Taghibiglou, C.: Primary blast-induced traumatic brain injury in rats leads to increased prion protein in plasma: A potential biomarker for blast-induced traumatic brain injury. J. Neurotrauma **32**, 58–65 (2015). doi:10.1089/neu.2014.3471
8. Sawyer, T.W., Wang, Y., Ritzel, D.V., Josey, T., Villanueva, M., Shei, Y., Nelson, P., Hennes, G., Weiss, T., Vair, C., Fan, C., Barnes, J.: High-fidelity simulation of primary blast: direct effects on the head. J. Neurotrauma **33**(13), 1181–1193 (2016). doi:10.1089/neu.2015.3914
9. Fournier, E., Sullivan, D., Bayne, T., Shewchenko, N.: Blast headform development, Defence R&D Canada, contract report CR 2007-234 (2007)
10. Ouellet, S., Bir, C., Bouamoul, A.: Direct comparison of the primary blast response of a physical head model with post-mortem human subjects. In: Defence R&D Canada, DRDC-RDDC-2014-P113 (2014)
11. Bouamoul, A., Ouellet, S.: A blast headform surrogate for the assessment of blast-induced traumatic brain injury. In: CTTSO/TSWG/PPE Symposium, Florida, USA, November 2012
12. Dionne, J.P., Nerenberg, J., Makris, A.: Reduction of Blast-Induced Concussive Injury Potential and Correlation with Predicted Blast Impulse. Med-Eng Sys Inc, Ottawa (2002)
13. Grujicic, M., Bell, W.C., Pandurangan, B., Glomski, P.S.: Fluid/structure interaction computational investigation of blast-wave mitigation efficacy of the advanced combat helmet. J. Mater. Eng. Perform. **20**(6), 877–893 (2011). doi:10.1007/s11665-010-9724-z
14. Nyein, M.K., Jason, A.M., Yu, L., Pita, C.M., Joannopoulos, J.D., Moore, D.F., Radovitzky, R.A.: In silico investigation of intracranial blast mitigation with relevance to military traumatic brain injury. Proc. Natl. Acad. Sci. **107**(48), 20703–20708 (2010). doi:10.1073/pnas.1014786107
15. Zhang, L., Makwana, R., Sharma, S.: Brain response to primary blast wave using validated finite element models of human head and advanced combat helmet. Front. Neurol. **4**, 1–12 (2013). doi:10.3389/fneur.2013.00088
16. Sarvghad-Moghaddam, H., Jazi, M.S., Rezaei, A., Karami, G., Ziejewski, M.: Examination of the protective roles of helmet/faceshield and directionality for human head under blast waves. Comput. Methods Biomech. Biomed. Eng. **18**(16), 1846–1855 (2015). doi:10.1080/10255842.2014.977878
17. Moss, W.C., King, M.J., Blackman, E.G.: Skull flexure from blast waves: A mechanism for brain injury with implications for helmet design. Phys. Rev. Lett. **103**, 108702 (2009). doi:10.1103/PhysRevLett.103.108702
18. Ganpule, S., Gu, L., Alai, A., Chandra, N.: Role of helmet in the mechanics of shock wave propagation under blast loading conditions. Comput. Methods Biomech. Biomed. Eng. **15**(11), 1233–1244 (2012). doi:10.1080/10255842.2011.597353
19. Panzer, M.B., Bass, C.R., Myers, B.S.: Numerical study on the role of helmet protection in blast brain injury. In: Proceedings of the Personal Armour Systems Symposium, Quebec City, Canada (2010)
20. Lockhart, P.A., Cronin, D.S.: Helmet liner evaluation to mitigate head response from primary blast exposure. Comput. Methods Biomech. Biomed. Eng. **18**(6), 635–645 (2015). doi:10.1080/10255842.2013.829460
21. Panzer, M.B., Myers, B.S., Bass, C.R.: Mesh considerations for finite element blast modeling in biomechanics. Comput. Methods Biomech. Biomed. Eng. **16**(6), 612–621 (2013). doi:10.1080/10255842.2011.629615
22. Singh, D., Cronin, D.S., Haladuick, T.H.: Head and brain response to blast using sagittal and transverse finite element models. Int. J. Numer. Methods Biomed. Eng. **30**(4), 470–489 (2014). doi:10.1002/cnm.2612
23. Kleiven, S.: Predictors for traumatic brain injuries evaluated through accident reconstructions. Stapp Car Crash J. **51**, 81–114 (2007)
24. Yang, K.H., Mao, H., Wagner, C., Zhu, F., Chou, C.C., King, A.I.: Modeling of the brain for injury prevention. Stud. Mechanobiol. Tissue Eng. Biomater. **3**, 69–120 (2011). doi:10.1007/8415_2010_62
25. Lockhart, P.A., Cronin, D., Williams, K., Ouellet, S.: Investigation of head response to blast loading. J. Trauma **70**(2), E29–36 (2011). doi:10.1097/TA.0b013e3181de3f4b
26. Cronin, D.S., Salisbury, C., Binette, J.S., Williams, K., Makris, A.: Numerical modeling of blast loading to the head. In: Proceedings of Personal Armour Systems Symposium, Brussels, Belgium, pp. 84–93 (2008)
27. Spitzer, V., Ackerman, M.J., Scherzinger, A.L., Whitlock, D.: The visible human male: a technical report. J. Am. Med. Inform. Assoc. **3**(2), 118–130 (1996). doi:10.1136/jamia.1996.96236280
28. Souli, M., Mahmadi, K., Aquelet, N.: ALE and fluid structure interaction. Mater. Sci. Forum **465**, 143–150 (2004). doi:10.4028/www.scientific.net/MSF.465-466.143
29. Hallquist, J.O.: LS-DYNA Theory Manual. Livermore Software Technology Corporation, Livermore (2006)
30. Bir, C.: Measuring blast-related intracranial pressure within the human head, US Army Medical Research Award Number W81XWH-09-1-0498 (2011)
31. Ouellet, S., Cronin, D., Worswick, M.: Compressive response of polymeric foams under quasi-static, medium and high strain rates conditions. Polym. Test. **25**, 731–743 (2006). doi:10.1016/j.polymertesting.2006.05.005
32. Gower, H.L., Cronin, D.S., Plumtree, A.: Ballistic impact response of laminated composite panels. Int. J. Impact Eng. **35**, 1000–1008 (2008). doi:10.1016/j.ijimpeng.2007.07.007
33. Thom, C.: Soft materials under air blast loading and their effect on primary blast injury. MASc. Thesis, University of Waterloo, Waterloo, ON, Canada (2009)
34. Singh, D.: Investigation of primary blast injury and protection using sagittal and transverse finite element head models. MASc. Thesis, University of Waterloo, Waterloo, ON, Canada (2015)